DEUTSCHES ELEKTRONEN-SYNCHROTRON

DESY 93-171
BI-TP 93/69
December 1993

The Interquark Potential: A QCD Lattice Analysis

K. D. Born
Institut für Theoretische Physik, RWTH Aachen

E. Laermann
Fakultät für Physik, Universität Bielefeld

R. Sommer, P. M. Zerwas
Deutsches Elektronen-Synchrotron DESY, Hamburg

T. F. Walsh
Physics Department, University of Minnesota, Minneapolis, USA

ISSN 0418-9833

NOTKESTRASSE 85 - 22603 HAMBURG

To be sure that your preprints are promptly included in the
HIGH ENERGY PHYSICS INDEX,
send them to (if possible by air mail):

DESY **Bibliothek** **Notkestraße 85** **22603 Hamburg** **Germany**	**DESY-IfH** **Bibliothek** **Platanenallee 6** **15738 Zeuthen** **Germany**

ISSN 0418-9833

DESY 93-171
BI-TP 93/69
December 1993

The Interquark Potential : A QCD Lattice Analysis

K. D. Born[1], E. Laermann[2], R. Sommer[3],
T. F. Walsh[4] and P. M. Zerwas[3]

[1]Inst. Theor. Physik, RWTH Aachen, D-52074 Aachen, FRG
[2]Fakultät für Physik, Universität Bielefeld, D-33501 Bielefeld, FRG
[3]Deutsches Elektronen-Synchrotron DESY, D-22603 Hamburg, FRG
[4]Physics Dept., Univ. of Minnesota, Minneapolis MN 55455

Abstract

We report on a QCD analysis of the potential between heavy quarks. Our calculation includes light quark loops and is carried out on a $16^3 \times 24$ lattice for couplings $\beta = 5.35$ and 5.15 and a quark mass $am_q = 0.010$. We generated lattice configurations using a hybrid Monte Carlo algorithm for $N_F = 4$ flavors of staggered fermions. We can explore distances between 0.12 fm and 0.9 fm for these parameters. The shape of the resulting potential is well described by the superposition of a term proportional to $1/R$ and a linear confinement potential. This full QCD potential is compared to results obtained from quenched approximation simulations on lattices of the same size and with the same value of the cutoff. We discuss a rough estimate of the QCD coupling.

1 Introduction

The potential between heavy quarks is an important nonperturbative QCD phenomenon. It is vital in understanding the phenomenology of quarkonium systems. The experimental analysis of charmonium and bottonium spectra has led to a detailed picture of the confining forces [1]. However, it still must be shown that the characteristic features of the phenomenological interquark potential can be derived from our microscopic theory of the strong interactions. Using the lattice formulation of QCD, the static potential has been extensively studied for the pure gluon theory without dynamical quarks [2, 3] (for earlier references see e.g. Ref. [4]). Only a few analyses have been carried out so far which address the problem of how virtual light quark loops affect the flux tube stretched between a heavy quark and antiquark [5, 6, 7].

Including dynamical quarks, we expect that the potential will be dominated by three different mechanisms at small, intermediate and large distances. At short distances perturbation theory will give a potential determined by one-gluon exchange, with an R dependent color charge as prescribed by asymptotic freedom. At intermediate distances (of the order of 0.5 fm) the potential rises linearly with the quark-antiquark separation. This feature can be extracted from charmonium and bottonium spectroscopy, which requires a string tension of $\sigma \approx 1\text{GeV/fm}$. For large distances > 1 fm, the color charges of the heavy quarks are expected to be screened by the spontaneous creation of the $q\bar{q}$ pairs possible with dynamical light quarks. As a result, heavy-light mesons $(Q\bar{q})$ can be created, and the interquark potential should flatten out at distances of the typical hadron size. (Eventually it will change to a Yukawa potential between the $(Q\bar{q})$ mesons when the separation is large enough.)

We report here on our measurement of the static potential in the presence of light dynamical quarks. Our couplings and lattice size restrict us to the intermediate range of distances between 0.12 fm and 0.9 fm. This is also the range probed by quarkonium systems. The analysis in full QCD is presented in some detail in section 2. In order to investigate the effects of dynamical quarks, we also compare our results in full QCD with quenched analyses at about the same values of lattice spacing and lattice size (section 3). In addition we present a rough estimate of the QCD coupling including quark-loop effects. We close with a discussion and conclusion in section 4.

2 The Static Quark Potential

Our analysis of the interquark potential is based on configurations generated by the MT_c Collaboration on $16^3 \times 24$ lattices. These configurations were produced by means of a hybrid Monte Carlo algorithm for $N_F = 4$ dynamical staggered quarks at coupling constants $\beta = 5.35$ and 5.15 for a quark mass of $ma = 0.01$ [8]. Our data set consists of 220 measurements at $\beta = 5.15$ and 200 at $\beta = 5.35$. In both cases the measurements are separated by two trajectories of length 1/2., The data were blocked over 40 trajectories while the integrated autocorrelation time was estimated to range from 10 to 40 trajectories, depending on the loop size. Small loops have the largest values of the integrated autocorrelation time. We have a limited number of effectively independent measurements. This affects the accuracy with which we can determine the error estimate.

As usual, we extract the potential from Wilson-loops with space extent $\vec{R}$ and time extent T in the form

$$V(\vec{R}) = -\lim_{T\to\infty} \frac{1}{T} \ln W(\vec{R}, T) \tag{1}$$

We endeavored to check the restoration of rotational symmetry. To do this, we computed, in addition to the loops with on-axis spatial paths, the 2- and 3-diagonal loops. This also extends the set of available distances $|\vec{R}|$ to larger and intermediate distances. This is useful as interpolating data.

To improve the projection of the Wilson-loop operator onto the $Q\bar{Q}$ ground state, we smeared the spacelike links according to a variant of the APE prescription [9]. A multihit type of procedure that would decrease the noise cannot be applied here, since the fermion determinant is part of the Boltzmann weight. Due to the smearing, the finite T approximants to the potential

$$V_T(\vec{R}) = -\frac{1}{a}[\ln W(\vec{R}, T) - \ln W(\vec{R}, T+a)] \tag{2}$$

are quite stable in T for $|\vec{R}|$ values less than $5a$. Here a denotes the lattice spacing. For definiteness, we have taken the potential from eq. (2) for $T = 4a$. We have compared the result with the potential as extracted from correlated χ^2 fits to the exponential fall-off in time, starting at $T_{min} = 4a$. We have found that fits with $t \geq 3a$ give reasonable χ^2 values in most cases, with agreement within errors. As an attempt to also account for the systematical uncertainties, our quoted errors on the fit parameters cover the differences between the two ways of extracting the potential.

It is well known that the potential at short distances contains significant lattice artifacts [10]. In analogy to the calculation of the force [3], we remove these artifacts *at*

tree level in the renormalized coupling through the definition

$$\begin{aligned} V_I(R_V) &= V(\vec{R}), \quad R_V \equiv [\,4\pi\,(G(\vec{R})]^{-1} \\ \text{with } G(\vec{R}) &= a^{-1} \int_{-\pi}^{\pi} \frac{d^3k}{(2\pi)^3} \frac{\prod_{j=1}^{3} \cos(R_j k_j/a)}{4\sum_{j=1}^{3} \sin^2(k_j/2)} . \end{aligned} \tag{3}$$

In principle, the potential defined in this way still depends on the orientation of $\vec{R}$. At our level of accuracy, we can neglect the effect of this direction dependence.

We find that the R dependence of the potential $V_I(R)$ is well fitted by a "Cornell" form

$$V_I(R) = c_0 - \frac{e}{R} + \sigma R \tag{4}$$

where c_0 accounts for self-energy contributions and σ denotes the string tension. The $1/R$ term may be physically due to one-gluon exchange at short distance, or vibrations of the QCD string at ranges where the string picture is appropriate [13]. In the latter case, e is predicted to have the value $e = \pi/12$.

The potentials at both values of β are dominated by a linear behavior beyond $R\sqrt{\sigma} = 3/4$. Fits to the data based on eq.(4) are most stable, for both values of β, when we fix the coefficient of the $1/R$ term to $\pi/12$ and omit the data points at the lowest quark-antiquark separations. Our results for the string tension from fits to distances $R \geq 0.3$ fm are given in Table 1. The central value for the ratio $\sqrt{\sigma}a(5.35)/\sqrt{\sigma}a(5.15) = 0.75(7)$ is surprisingly (and probably accidentally) close to the 2-loop prediction of asymptotic scaling, which amounts to 0.74 at zero quark mass. Taking these results for the string

β	e	σ
5.15	$\pi/12$	0.103(16)
5.35	$\pi/12$	0.057(7)

Table 1: *Results in full QCD for the string tension in lattice units at the two couplings analyzed in this study. The coefficient of the* $1/R$ *term has been kept fixed. Only data for* $R \geq 0.3$ *fm were used in the fit.*

tension in lattice units, we find a lattice spacing $a = 0.114(6)$ fm at $\beta = 5.35$ and $a = 0.153(11)$ fm at $\beta = 5.15$, provided the physical value for the string tension, $\sqrt{\sigma} = 420$ MeV, is used to set the scale. On the other hand, we may equally well take the lattice spacing from the measured vector meson masses [11]. Since these masses are determined at non-zero values of the quark masses, we use the approximate relation $m_V = 770MeV + 396MeV * (m_{PS}/m_V)^2$, obtained from the experimental ρ, K^* and the π, K masses, and the measured pseudoscalar to vector meson mass ratios. In this way

we arrive at a physical string tension $\sqrt{\sigma} = 400(25)$ MeV and $\sqrt{\sigma} = 360(30)$ MeV at $\beta = 5.35$ and 5.15 respectively.

These results are summarized in Fig. 1, where we plot the potentials from both couplings in physical units obtained from the string tension. (The potentials have been computed for slightly different quark mass, $m_q^{RGI} \approx 48$ MeV and 33 MeV at $\beta = 5.35$ and 5.15. However, in this narrow interval we could not see a dependence on the quark mass in the data.)

The shape of the lattice potential, as well as the approximate match of the lattice spacings from the vector meson mass with that from the string tension when the potential is fitted to eq.(4), indicate that the potential does not yet flatten out at distances up to ≈ 0.9 fm. It is possible to obtain an upper bound to the distance at which the potential should turn over. This can be provided through a determination of the binding energy in a bound state of a heavy and a light quark. Calculations of this quantity in the quenched approximation [12] suggest that the energy of two heavy-light mesons must become smaller than the energy stored in the flux tube at distances around 1.9 fm.

Turning to the potential at small distances, we have already mentioned that good fits to the data are obtained when the coefficient of the $1/R$ term is fixed to $e = \pi/12$, with the data points at the shortest quark-antiquark separations omitted from the fit. This value of e is motivated by a string picture of the flux tube where the $1/R$ term describes the vibrations of a thin string [13]; it is a typical long range effect. At small R, we enter into the region where lattice artifacts are potentially large. (However, they should be considerably reduced by using the tree-level improved observable V_I.) If we include the small distances into a fit to eq.(4), we do not observe a significant deviation of the coefficient e away from $e = \pi/12$.

From the force, which will be discussed later in detail, we can define a renormalized coupling $\alpha_{q\bar{q}}(R) = \frac{3}{4}F(R)R^2$. In an exploratory spirit, we have taken $\alpha_{q\bar{q}}(R)$ at $Rm_\rho \sim 1$, changed it to the $\overline{MS}$ scheme and evolved it to the Z mass energy scale. (We used the 2–loop β–function with $n_f = 4$ flavors and $n_f = 5$ flavors beyond 5 GeV.) From this, we get $\alpha_{\overline{MS}}(M_Z) \sim 0.11$ to 0.12. Since we *assumed* that perturbation theory is valid already at very low energies – we start from a value $\alpha_{q\bar{q}} \sim 0.5$ – we cannot give an error estimate. Nevertheless, it is interesting that $\alpha_{\overline{MS}}(M_Z)$ is roughly of the size expected.

We also performed a fit to a QCD inspired potential [14], with a Coulomb coefficient $e = \frac{4}{3}\alpha(R)$ depending on the distance as predicted by perturbative QCD [15]. This fit returns a value with acceptable χ^2 and which translates into $\alpha_{\overline{MS}}(M_Z) \approx 0.105$ [1]. Clearly,

[1]This number might be compared to a determination of $\alpha_{\overline{MS}}(M_Z)$ from the long-range behavior of the potential, by means of the asymptotic β function in terms of an improved coupling [16]. Here we obtain a value of $\alpha_{\overline{MS}}(M_Z) \approx 0.11$.

more data at smaller lattice spacings are needed in order to establish the perturbative behavior at small quark-antiquark separations and to obtain a trustworthy error estimate for the coupling.

3 A Comparison to Quenched Potentials

In order to assess the effects of dynamical fermions on the potential, and to investigate possible differences compared to the quenched case, we carried out a quenched analysis on lattices of the same size, $16^3 \times 24$. We chose couplings $\beta = 5.7, 5.8, 5.9$ and 6.0. We expect values for the lattice spacing in physical units to be similar to those in the unquenched simulation. We employed an overrelaxed algorithm (OR) with 1 Metropolis step every 5 OR sweeps. For each β we allowed 2000 sweeps for thermalization and collected about 100 configurations, separated by 50 sweeps.

The Wilson loops on the quenched configurations are of good statistical quality, with autocorrelation times $\mathcal{O}(1)$ per measurement, compared to $\mathcal{O}(10-40)$ trajectories in the unquenched case. The plateaux in the ratio of time-consecutive loops can now be followed to larger T values for all R. The potential was extracted using the same methods as described in section 2.

The potential is very well described by a superposition of a Coulomb and a linear term. Again, the fit results are most stable when the coefficient of the $1/R$ term is fixed to $\pi/12$ while the data points at small R are omitted from the fit. The values are collected in Table 2.

β	5.70	5.80	5.90	6.00
σa^2	0.161(7)	0.108(3)	0.070(2)	0.051(2)

Table 2: *Fit parameters for the string tension in lattice units for the quenched simulations. α has been fixed to $\pi/12$ and data below $R = 0.3$ fm were omitted from the fit.*

In order to compare the results of full and quenched QCD, we first looked at the β shifts necessary to bring quenched and full QCD data on top of each other. One might argue that the onset of screening effects shows up first in the Wilson loops [7] as a loop size dependence of $\Delta\beta = \beta^{quenched}_{equivalent} - \beta^{full}$. Indeed, comparing the logarithms of Wilson loops directly and determining the equivalent quenched β values, we do observe a marked loop-size dependence, Table 4. However, the Wilson loops include non-scaling pieces which dominate at small distances. These contributions fake screening effects. It

	Table 4			
R	T = 1	T = 2	T = 3	T = 4
1.000	0.405(16)	0.421(10)	0.428(08)	0.432(07)
1.414	0.416(13)	0.435(08)	0.444(06)	0.449(06)
1.732	0.424(19)	0.444(10)	0.455(08)	0.463(07)
2.000	0.439(20)	0.457(10)	0.469(08)	0.476(07)
2.828	0.442(18)	0.470(09)	0.487(07)	0.496(06)
3.000	0.457(21)	0.482(10)	0.496(08)	0.504(07)
3.464	0.446(23)	0.479(13)	0.496(10)	0.504(09)
4.000	0.472(25)	0.497(14)	0.511(11)	0.519(10)
4.243	0.453(26)	0.488(13)	0.507(11)	0.517(10)
5.196	0.456(27)	0.494(14)	0.513(11)	0.523(10)
5.657	0.463(27)	0.499(14)	0.517(11)	0.527(09)
6.928	0.464(30)	0.505(17)	0.520(14)	0.528(12)

Table 3: *β shifts of planar Wilson loops for $\beta = 5.35$. The loops are not symmetric in R and T because we smeared the spatial links.*

is thus necessary to isolate and subtract this part, i.e. to compare only the physical part of the Wilson loop, the potential.

For this purpose, we extract the shifts in β which map the string tensions onto each other from Tables 1 and 2 . The results are 0.67(4) at $\beta = 5.15$ and 0.61(4) at 5.35, based on linear interpolations in β between $\ln \sqrt{\sigma}$. (Note the difference with the $\Delta\beta$ values obtained from the Wilson loops, i.e. the influence of self-energies.) Keeping in mind that the π/ρ mass ratios at $ma = 0.01$ – and thus the physical quark masses – are not precisely the same in the full and the quenched simulations [17, 11], the β shifts in the potential are not in disagreement with the equivalent shifts in the quark condensate at $ma = 0.01$, 0.59(1) and 0.57(1), respectively. In addition, we interpolated available quenched data on the ρ mass [18] to the same m_π/m_ρ ratios as in our full QCD runs [11], assuming that m_ρ and m_π^2 depend linearly on the quark mass. (The interpolation in β was logarithmic.) Then we can determine the β shifts at the same physical quark mass. From the appropriate vector meson mass at this ratio, we obtain for $\beta = 5.35$ and $m_{PS}/m_V = 0.387$ a β shift of $\Delta\beta = 0.63(3)$, while for $\beta = 5.35$ and $m_{PS}/m_V = 0.508$ the result is $\Delta\beta = 0.60(2)$. Again, a mismatch could have indicated i) the onset of screening effects, ii) a different physical value for the string tension and iii) effects of a finite lattice spacing. We have no evidence for any such effect.

Note that the shift in the location of the chiral/deconfinement transition, β_c, is considerably larger, i.e., in contrast to the above observables, the transition temperature is significantly influenced by dynamical fermions [19].

Comparing the potentials directly, it is clear from the fit results that both sets of

data can be mapped onto each other very well provided the string tension is used to set the scale and the self-energies are properly adjusted. The same holds true when the vector meson mass at fixed m_{PS}/m_V ratio is used. Alternatively, we compared the force in full and quenched QCD

$$\bar{F}(R_F) = \frac{V(\vec{R}+\vec{d}) - V(\vec{R})}{|\vec{d}|} \tag{5}$$

For the intermediate distance R_F we adopted the prescription [3]

$$R_F = \left(4\pi \frac{G(\vec{R}+\vec{d}) - G(\vec{R})}{|\vec{d}|} \right)^{-1/2} \tag{6}$$

such that $F(R_F)$ is a tree-level improved observable. (For the linear part of the potential the exact definition of R_F is of course not important.) In contrast to the potential, the forces can be compared directly once a common scale is chosen – the ρ mass, for example. It is not necessary to perform a fit to the potential in order to subtract the self-energies. In this way, correlations between the fit parameters can be avoided. We again took the vector meson mass at fixed pseudoscalar to vector meson mass ratio m_{PS}/m_V [11, 18] as our mass scale. In Fig. 2 we plot the dimensionless quantities $R^2F(R)$ *vs* Rm_V for $\beta^{full} = 5.35$, compared to the quenched data at $\beta^{quenched} = 5.90$ and 6.00.

The data is somewhat noisy because the error on the force is dominated by the potential results at the larger distances. Still, the data confirm our conclusion that at a fixed value of the lattice spacing there is no difference between quenched and full QCD within our errors. This is particularly remarkable since the quenched results alone show a significant dependence on the cutoff. To this end we note, that the $\beta = 5.7$ results fall significantly below the points plotted in Fig. 2.

Finally, we list the results for the ratio of the string tension to the vector meson mass at fixed m_{PS}/m_V in Table 4. Comparing various quenched β values, (known) scaling violations are apparent. However, comparing full and quenched QCD at the appropriate vector meson mass or string tension in lattice units, no difference in their ratio is visible. So we observe that, at a fixed value of the cutoff and within our precision, this ratio is not affected by the four flavors of dynamical quarks.

4 Conclusion

Using a lattice simulation, we have analyzed the static potential between heavy quarks in full QCD including four flavors of dynamical staggered quarks. The potential is well

	$m_{PS}/m_V = 0.387$			$m_{PS}/m_V = 0.508$		
β	$m_V a$	$a\sqrt{\sigma}$	$\sqrt{\sigma}/m_V$	$m_V a$	$a\sqrt{\sigma}$	$\sqrt{\sigma}/m_V$
5.70	0.92(5)	0.401(9)	0.44(3)	1.00(4)		0.40(2)
5.80	0.71(2)	0.329(5)	0.46(2)	0.76(2)		0.43(2)
5.90	0.56(2)	0.265(4)	0.47(2)	0.59(2)		0.45(2)
6.00	0.42(2)	0.226(5)	0.54(3)	0.45(2)		0.50(3)
5.15	0.75(2)	0.321(24)	0.43(3)			
5.35				0.52(1)	0.239(14)	0.46(3)

Table 4: *Vector meson mass, (square root of) the string tension and their ratio, at fixed pseudoscalar-to-vector meson mass ratio.*

described by a superposition of a Coulomb term plus a linear confinement potential in the quark separation range 0.12 fm $\leq R \leq$ 0.9 fm. Within this range, the observed shape of the potential is in accord with heavy quarkonium spectroscopy. A screening behavior does not set in at distances up to $\leq$ 0.9 fm. When the data for small quark-antiquark separations are omitted, the strength e of the Coulomb term comes out close to the value $\pi/12$ predicted in effective string field theories. Below $R \leq 0.3$ fm the data can be parametrized by a perturbative ansatz, but more data at smaller lattice spacings are needed to firmly establish this. Taken at face value, our analyis leads to $\alpha_{\overline{MS}}(M_Z) \sim 0.11$ for five flavors of dynamical quarks.

The comparison with results from a related quenched analysis yields the following picture. At a fixed value of the cutoff, e.g. $m_V a = 0.52$, the presence of dynamical quarks leads to small effects (below our statistical precision) in the force between static quarks. Apart from the screening of the bare charge (an overall β-shift) no physical effect of dynamical quarks is visible. This observation is relevant to continuum QCD, since we have investigated distances $R << 1/m_q$ and momenta large compared to our quark masses. We believe that this allows our conclusions to apply to the real case of vanishing quark mass.

Note added. After finalizing this letter we received a paper [20] in which the interquark potential for 2 quark flavors has been analyzed; the conclusions are similar.

References

[1] W. Buchmüller and S. Cooper, in *"High Energy Electron-Positron Physics"*, eds. A. Ali and P. Söding, World Scientific, Singapore 1989.

[2] C. Michael, Phys. Lett. B283 (1992) 103;
S. P. Booth *et al.* (UKQCD Collaboration), Phys. Lett. B294 (1992) 385;
G. Bali and K. Schilling, Phys. Rev. D46 (1992) 2636, D47 (1993) 661.

[3] R. Sommer, preprint DESY 93-062 and Nucl. Phys. B in press.

[4] E. Laermann, in *"QCD – 20 Years Later"*, eds. P. M. Zerwas and H. A. Kastrup, World Scientific, Singapore 1993.

[5] E. Laermann *et al.*, Phys. Lett. B173 (1986) 437.

[6] M. Fukugita *et al.*, Phys. Lett. B191 (1987) 164;
M. Campostrini *et al.*, Phys. Lett. B193 (1987) 78;
K.D. Born *et al.*, Phys. Rev. D40 (1990) 1653.

[7] R. Gupta *et al*, Phys. Rev. D44 (1991) 3272.

[8] R. Altmeyer *et al.* (MT_c Collaboration), Nucl. Phys. B(Proc. Suppl.)20 (1991) 380.

[9] M. Albanese *et al.* (APE Collaboration), Phys. Lett. B192 (1987) 163.

[10] C. B. Lang and C. Rebbi, Phys. Lett. B115 (1982) 137.

[11] R. Altmeyer *et al.* (MT_c Collaboration), Nucl. Phys. B389 (1993) 445.

[12] C. Alexandrou *et al.*, preprint PSI-PR-92-27 and Nucl. Phys. B in press.

[13] M. Lüscher, Nucl. Phys. B180 (1981) 317.

[14] M. J. Strassler and M. E. Peskin, Phys. Rev. D43 (1991) 1500.

[15] W. Fischler, Nucl. Phys. B129 (1977) 157;
A. Billoire, Phys. Lett. B104 (1981) 472.

[16] J. Fingberg, U. Heller and F. Karsch, Nucl Phys. B392 (1993) 493;
see also P. Lepage and P. Mackenzie, Phys. Rev. D48 (1993) 2250.

[17] R. Altmeyer *et al.* (MT_c Collaboration), Nucl. Phys. B(Proc. Suppl.)20 (1991) 394.

[18] S. Cabasino *et al.* (APE Collaboration), Nucl. Phys. B343 (1990) 228;
R. Gupta *et al.*, Phys. Rev. D43 (1991) 2003;
K. M. Bitar *et al.* (HEMCGC Collaboration), Nucl. Phys. B(Proc. Suppl.)20 (1991) 362.

[19] R. Gavai *et al.* (MT_c Collaboration), Phys. Lett. B241 (1990) 567.

[20] U. M. Heller *et al.* (HEMCGC Collaboration), Preprint FSU-SCRI-94-09.

Figure Captions

Fig. 1 : The interquark potential measured for two values $\beta = 5.15$ and $\beta = 5.35$ and mapped onto each other by setting the scale from the fitted string tension.

Fig. 2 : The forces in full and quenched QCD at $\beta = 5.35$ and 5.90 respectively, normalized to the vector meson mass at fixed m_{PS}/m_V ratio.

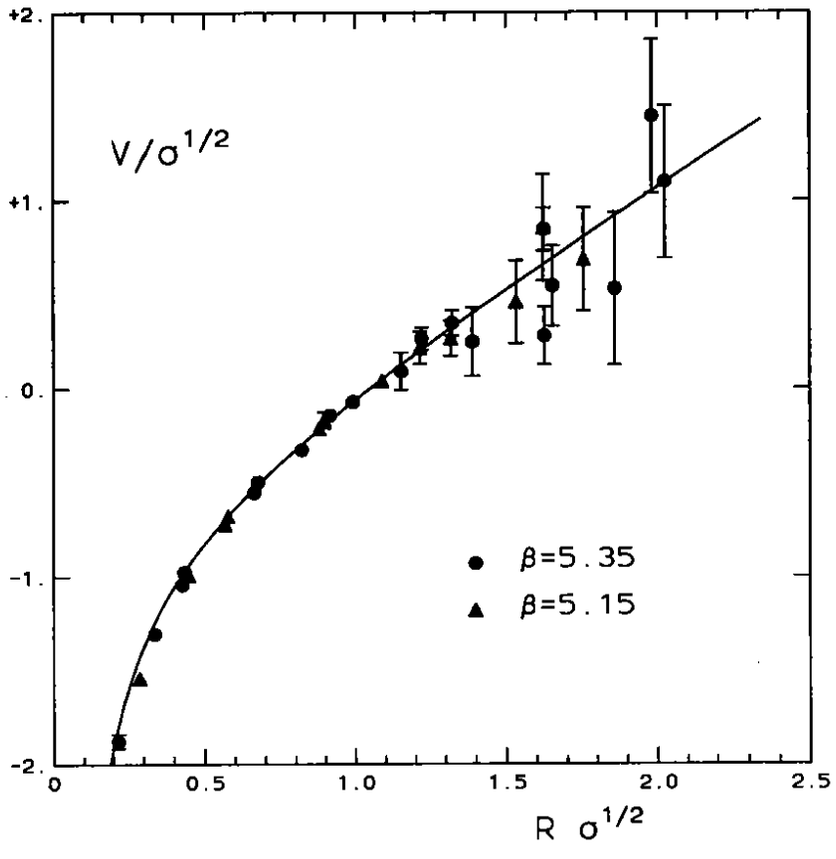
+2.
+1.
0.
-1.
-2.
0
0.5
1.0
1.5
2.0
2.5
$V/\sigma^{1/2}$
$R\ \sigma^{1/2}$
β=5.35
β=5.15

Fig. 1.

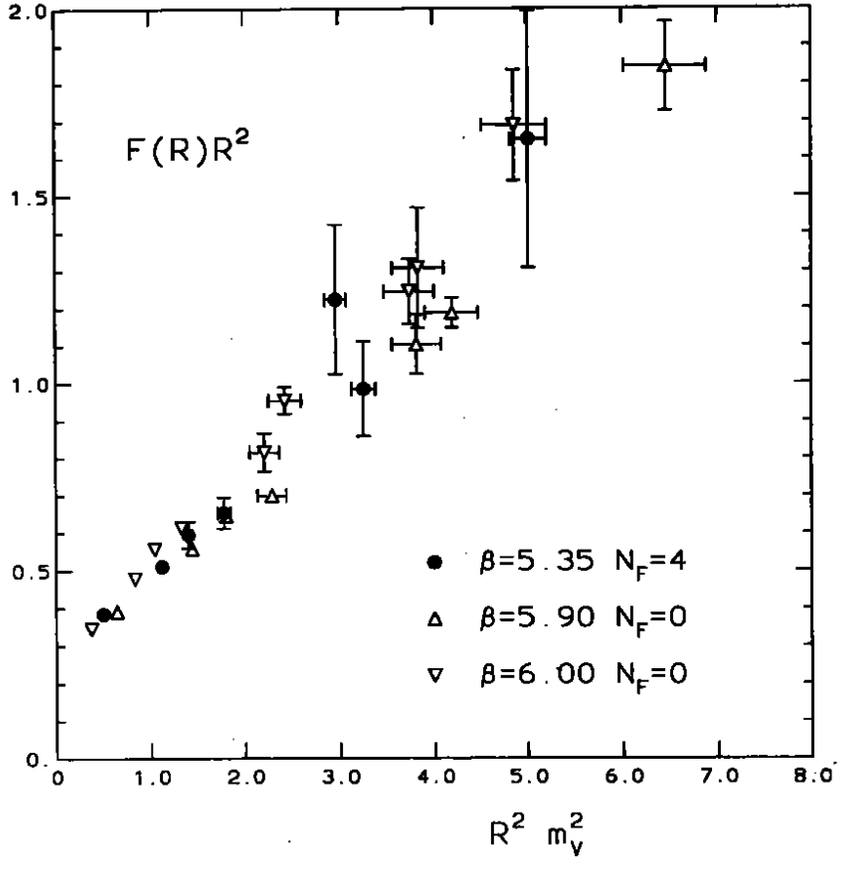
2.0
1.5
1.0
0.5
0.
0
1.0
2.0
3.0
4.0
5.0
6.0
7.0
8.0
$F(R)R^2$
$R^2\ m_v^2$
β=5.35 N_F=4
β=5.90 N_F=0
β=6.00 N_F=0

Fig. 2.